Robotica (2014) volume 32, pp. 1125–1134. © Cambridge University Press 2014
doi:10.1017/S0263574713001288

Torque distribution optimization of redundantly actuated planar parallel mechanisms based on a null-space solution

Jung Hyun Choi†, TaeWon Seo† and Jeh Won Lee*

School of Mechanical Engineering, Yeungnam University, Gyeongsan 712-749, Republic of Korea

(Accepted December 12, 2013. First published online: January 15, 2014)

SUMMARY

Redundant actuation for the parallel kinematic machine (PKM) is a well-known technique for overcoming general drawbacks of the PKM by helping it to avoid singularity and enhance stiffness characteristics, among others. Torque distribution plays a critical role in redundant actuation because this actuation causes the PKM to consume too much energy or put a substantial amount of stress on joints and links. This paper proposes a new torque distribution method for reducing the maximum torque of the actuator of a planar PKM. Here the main idea behind the proposed method is the use of superposition of a particular solution for a non-redundant case and an optimized null-space solution for a redundant case with a constant coefficient. The optimal value of a null-space solution can be easily determined by checking only the intersection points of the profile of the actuator's torque as the coefficient varies. We consider three cases of planar PKMs—2-, 3-, and 4-RRR PKMs—and present a detailed procedure for deriving a kinematic solution for the 2-RRR PKM based on Screw theory. We compare the proposed method with the minimum-norm pseudo-inverse method and assess a limitation of the proposed method. The torque distribution algorithm can be used to determine the number of actuators in an efficient manner and to reduce energy consumption.

KEYWORDS: Torque distribution; Optimization; Redundant actuation; Parallel mechanism; Particular solution; Null-space solution.

1. Introduction

Redundant actuation is a technique for enhancing the characteristics of the parallel kinematic machine (PKM).[1,2] Many studies have reported that redundant actuation can help PKMs avoid a singularity configuration[3] or enhance stiffness characteristics.[4] Because a redundantly actuated PKM has more actuators than the degree of freedom (DOF) of the PKM, the controller can use redundant actuators to change the characteristics of the PKM.

Redundant actuation has some drawbacks from the existence of internal torque. Several studies have attempted to overcome a decrease in the PKM's accuracy resulting from internal torque. Jeong *et al.*[5] present a calibration method by considering the joint indexing error from internal torque on each joint. Jeon *et al.*[6] calibrate the positioning error from the internal torque of a redundant PKM by using a simple projection method. It is well known that internal torque can change stiffness characteristics in an effective manner but that it can also cause a positioning error for the end-effector.

Another drawback of redundant actuation is a large amount of energy consumption arising from the existence of additional actuators and internal torque. Here a torque distribution method can be very useful for reducing energy and torque consumption. The pseudo-inverse method[7] and the weighted pseudo-inverse method[8] are widely used to obtain minimum-norm torque distribution. Shim *et al.*[9] propose a new torque distribution method for reducing the minmax value of actuator torque based on the geometrical approach of Screw theory. Kim[10] shows that energy can even be reduced by redundant actuation through the use of negative work when the end-effector moves in the direction of gravity.

* Corresponding author. E-mail: jwlee@yu.ac.kr
† The authors contributed equally as co-first authors.

There are several important researches on torque distribution of non-redundant actuations. Ma and Hirose[11] introduce two methods of damped squared-torque optimization and damped null-space torque optimization to improve the local torque optimization techniques. They verified the algorithm by simulation. Several local and global optimization algorithms on torque distribution have been proposed by Suh and Hollerbach.[12] Maciejewski[13] presents torque minimization of redundant manipulators by using singular value decomposition technique. Nokleby *et al.*[14] introduce scaling factors to examine force capabilities of non-redundant and redundant parallel manipulators.

This paper proposes a new torque distribution method that can help a redundantly actuated PKM to minimize the maximum actuator torque. Based on the Jacobian relationship, we derive a solution by combining a particular solution for a non-redundant case with a null-space solution for a redundant case with a constant coefficient. We optimize the null-space solution by changing the coefficient and determine an optimal solution by checking only the intersection points of actuator torque according to the coefficient. For case studies, we analyze three redundant PKMs with the revolute (R) joint—2-RRR,[15] 3-RRR,[9,16] and 4-RRR[17] PKMs—and derive a Jacobian matrix of the mechanisms through Screw theory, which is a geometrically intuitive method for calculating the kinematics of manipulators.[18]

Two main contributions of the research can be summarized as follows:

- Computation is very efficient. Since the algorithm finds optimal value by only vertex search on the defined region, the computing takes very little time. We believe the algorithm can be very efficient in real-time applications.
- Minmax value of the actuator torque is determined on pre-defined trajectories. By changing the null-space solution, the maximum absolute values of actuator torques are minimized along a pre-defined trajectory. In design process, the size of actuators can be optimally determined by the proposed algorithm.

The rest of this paper is organized as follows: Section 2 describes the proposed torque distribution algorithm. Section 3 examines the 2-RRR PKM, details the derivation of the Jacobian matrix through Screw theory, and provides a singularity analysis based on the matrix. Section 4 considers 3- and 4-RRR PKMs and Section 5 concludes with a discussion on the limitation of the proposed algorithm.

2. Torque Distribution Algorithm

The torque distribution of a redundant PKM plays a critical role in reducing energy consumption and internal torque. In general, there is no unique solution to the torque distribution problem of a redundant PKM because the number of actuators exceeds that of the DOF of the PKM. Here, through the use of the remaining DOF of actuators, various end-effector characteristics, such as stiffness, can be changed. In addition, operating torque can be changed while the end-effector maintains constant external force.

The wrench of the end-effector ($\hat{w}$) and actuator torque (λ) has the following relationship:

$$\hat{w} = j\lambda, \tag{1}$$

where j denotes the Jacobian matrix of the mechanism. It should be noted that the number of columns of j always exceeds that of rows of j in a redundant PKM. In a non-redundant case, the number of columns equals that of rows.

This paper determines actuator torque while the wrench of the end-effector is maintained as a constant. The paper's optimization problem can be expressed as follows:

$$\text{Find } \lambda \text{ to minimize } \max(|\lambda_i|) \text{ along a predefined path}, \tag{2}$$

where λ_i indicates the components of the vector λ. The objective function of the problem can reduce the maximum number of actuators, which means that actuators can be determined in an efficient manner in the design process and can be operated with a small amount of energy.

https://doi.org/10.1017/S0263574713001288 Published online by Cambridge University Press

We start by calculating a general solution to Eq. (1). Using some linear algebra, we assume the following general solution:

$$\lambda = \lambda_p + c\lambda_n. \tag{3}$$

Here, λ_p and λ_n can be calculated as follows. λ_p is a particular solution to a reduced non-redundant problem as follows:

$$\hat{w}_p = j_{sq}\lambda_p, \tag{4}$$

where j_{sq} is the square Jacobian matrix by eliminating columns of redundant actuations, and λ_n is a null-space solution to Eq. (1) as follows:

$$j\lambda_n = 0. \tag{5}$$

In Eq. (3), λ can be calculated by using c which is a constant for a linear combination of these two solutions. To calculate λ_p, we set the columns of redundancy from differences between the number of actuators and that of the DOF of the end-effector to zero vectors until these two numbers are equal. Any column of redundancy can be set to zero in this algorithm, and we set the last column to zero vectors in the case studies. Note that we can easily calculate the null-space vector of λ_n of Eq. (5) by the row echelon form of the Jacobian matrix.[19]

Here the main idea is changing c effectively to determine λ. In general, an optimal search requires many iterations to determine the final solution. In this paper, we assume a general solution as a linear combination of a particular solution and a null-space solution with a constant coefficient, and therefore it is sufficient to search only for an intersected vertex to determine an optimal solution. Note that in the multi-variable linear search method, an optimal solution is not in the middle of the line but is always in the intersections. This method can sharply reduce the computation time and thus is very effective in achieving real-time operations.

In sum, the proposed method is based on a general solution composed of a particular solution for a non-redundant case and a null-space solution for a redundant case. By changing the coefficient for the null-space solution, we determine an optimal solution for minimum actuator torque through the use of a simple intersection-searching method. Here it needs to be emphasized that this simple and fast method is very efficient in determining an optimal solution for real-time applications.

3. Case Study I: The 2-RRR PKM

In this section, we analyze the 2-RRR redundant PKM based on the proposed torque distribution algorithm. We conduct a kinematic analysis based on Screw theory to calculate the Jacobian matrix and use the matrix to determine torque distribution. We compare the results for the proposed algorithm with those for the minimum-norm method and a non-redundant case.

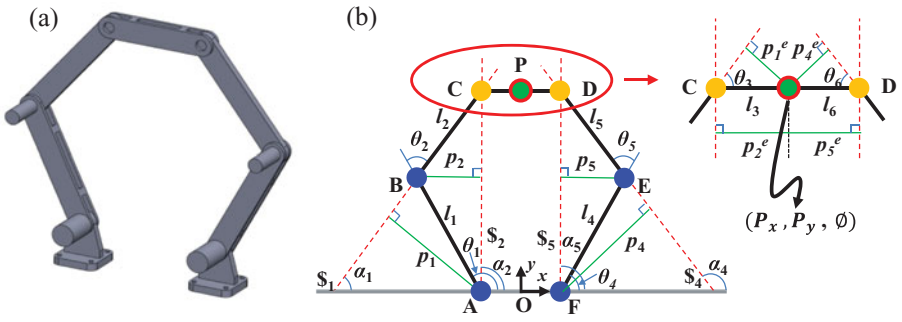

Fig. 1. (Colour online) Redundantly actuated 2-RRR PKM and the kinematic configuration: (a) the redundant 2-RRR PKM and (b) a kinematic configuration for the kinematic analysis. A, B, E, and F indicate the positions of actuators, and C and D indicate the positions of passive joints. (P_x, P_y, φ) is the pose of the end-effector, l_i is the length of the link, and θ is the angle between links. Other symbols are defined in the main text during derivations.

https://doi.org/10.1017/S0263574713001288 Published online by Cambridge University Press

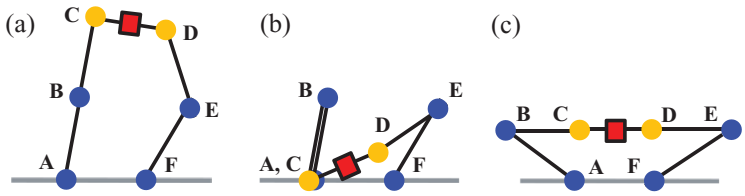

Fig. 2. (Colour online) Singularity configuration of the 2-RRR PKM: (a) $p_1 = p_2 = 0$ (the $p_4 = p_5 = 0$ case is also singularity configuration, which is not shown in this figure.); (b) $p_1 = 0$ (the $p_4 = 0$ case is also singularity); and (c) no singularity through redundant actuation.

Table I. Components of the Jacobian matrix in Eq. (6).

Sym.	Value	Sym.	Value	Sym.	Value	Sym.	Value
α_1	$\theta_1 + \theta_2$	p_1^e	$l_3 \sin\theta_3$	p_1	$l_1 \sin\theta_2$	l_{lc}	$\sqrt{l_1^2 + l_2^2 + 2l_1 l_2 \cos\theta_2}$
α_2	$\arctan\frac{l_1 s_1 + l_2 s_{12}}{l_1 c_1 + l_2 c_{12}}$	p_2^e	$l_3 \sin(\phi_3 - \alpha_1)$	p_2	$l_1 l_2 \sin\theta_2 / l_{lc}$	l_{rc}	$\sqrt{l_4^2 + l_5^2 + 2l_4 l_5 \cos\theta_5}$
α_3	$\theta_4 + \theta_5$	p_4^e	$l_6 \sin\theta_6$	p_4	$l_4 \sin\theta_5$	ϕ_3	$\theta_1 + \theta_2 + \theta_3$
α_4	$\arctan\frac{l_4 s_4 + l_5 s_{45}}{l_4 c_4 + l_5 c_{45}}$	p_5^e	$l_6 \sin(\phi_6 - \alpha_2)$-	p_5	$l_4 l_5 \sin\theta_5 / l_{rc}$	ϕ_6	$\theta_4 + \theta_5 + \theta_6$

3.1. Mechanism description

Figure 1 shows the redundant 2-RRR PKM and its kinematic configuration. The mechanism has four actuators to achieve three DOFs for the end-effector. We use the Jacobian matrix to examine the relationship between actuator torque and the wrench of the end-effector. In addition, we determine the matrix based on Screw theory[18] and define a singularity configuration. Choi and Lee[20] provide a kinematic analysis of a 2-RRR PKM, and Spong *et al.*[21] verify the results of this analysis by comparing them with those of a conventional kinematic analysis.

3.2. Kinematic analysis

In general, the wrench of the end-effector is defined based on the screw vector and the linear force because of actuators[16]:

$$\hat{w} = \bar{j}\bar{\lambda}, \tag{6}$$

where $\bar{j}$ is a Jacobian matrix composed of the screw vector and expressed as $\left[\$_1\ \$_2\ \$_4\ \$_5\right]$ and $\bar{\lambda}$ is the linear force along the screw vector and expressed as $\left[f_1\ f_2\ f_3\ f_4\right]^T$. Each screw vector is defined using cosine and sine functions and the perpendicular distance from the end-effector as follows:

$$\$_i = \left[c_{\alpha i} \quad s_{\alpha i} \quad p_i^e\right]^T, \tag{7}$$

where $c_{\alpha i}$ and $s_{\alpha i}$ are cosine and sine functions of α_i, respectively, and p_i^e is the perpendicular distance between the screw vector and the end-effector.

Because the relationship between the force and torque is $f_i = \tau_i / p_i$, where p_i is the distance between the screw and the actuator, we can determine j in Eq. (1) as follows:

$$j = \begin{bmatrix} \frac{c_{\alpha 1}}{p_1} & \frac{c_{\alpha 2}}{p_2} & \frac{c_{\alpha 4}}{p_4} & \frac{c_{\alpha 5}}{p_5} \\ \frac{s_{\alpha 1}}{p_1} & \frac{s_{\alpha 2}}{p_2} & \frac{s_{\alpha 4}}{p_4} & \frac{s_{\alpha 5}}{p_5} \\ \frac{p_1^e}{p_1} & \frac{p_2^e}{p_2} & \frac{p_4^e}{p_4} & \frac{p_5^e}{p_5} \end{bmatrix}, \tag{8}$$

where the components of j are arranged in Table I.

Two types of singularity occur in the redundant 2-RRR PKM. We can determine singularity from the screw components of j. Figure 2(a) shows that the first type of singularity occurs when

https://doi.org/10.1017/S0263574713001288 Published online by Cambridge University Press

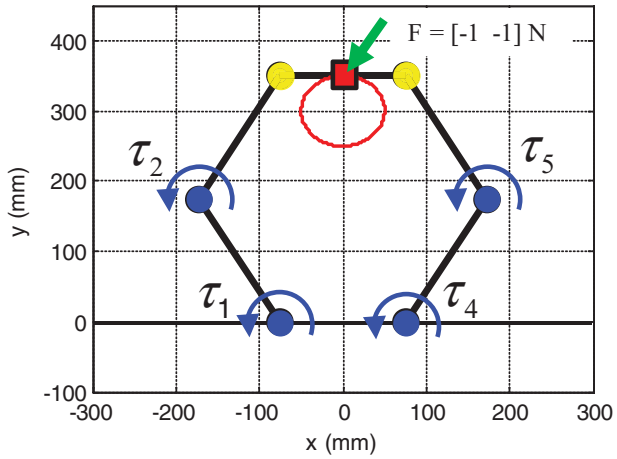

Fig. 3. (Colour online) Trajectory and external force for optimization—blue circles denote actuators and yellow circles, passive joints. The red line is the test trajectory of the end-effector and the green arrow indicates the application of an external force of [-1 -1] N. $l_1 = l_2 = l_4 = l_5 = 200$ mm and $l_3 = l_6 = 75$ mm are used in the simulation. The distance between τ_1 and τ_2 is 150 mm.

$p_1 = p_2 = 0$. As shown in Eq. (8), the first two columns of j go to infinity when $p_1 = p_2 = 0$, and therefore j is not well defined. Here $p_4 = p_5 = 0$ reflects the same singularity configuration. Figure 2(b) shows that the second type of singularity occurs when $p_1 = 0$. Note that these two types of singularity are exactly coincident with the inverse kinematic singularity of the end-effector in ref. [22]. The forward kinematic singularity, as in Fig. 2(c), can be avoided by using redundant actuation.

3.3. Torque distribution results

Based on the torque distribution algorithm in Section 2 and the Jacobian matrix in Section 3.2, we simulate torque distribution for the 2-RRR PKM. To calculate optimal torque, we calculate λ_p from a reduced 3×3 non-redundant problem in which the last column of j is set to zero. We calculate λ_n by the row echelon form of a 3×4 Jacobian matrix. Figure 3 shows the geometric parameters and notations of torque. When the end-effector follows the red circular line, the end-effector can maintain an external force of [-1 -1] N.

In the proposed algorithm, we perform torque distribution by combining a particular solution and a null-space solution as Eq. (3). The particular solution is determined by Eq. (4), where j_{sq} is obtained by eliminating the last column of the non-square Jacobian matrix as follows:

$$j = \begin{bmatrix} j_{11} & j_{21} & j_{31} & j_{41} \\ j_{12} & j_{22} & j_{32} & j_{42} \\ j_{13} & j_{23} & j_{33} & j_{43} \end{bmatrix} \text{ and } j_{sq} = \begin{bmatrix} j_{11} & j_{21} & j_{31} \\ j_{12} & j_{22} & j_{32} \\ j_{13} & j_{23} & j_{33} \end{bmatrix}. \tag{9}$$

Then, we can determine $\lambda_p$by adding zero to meet the dimension as follows:

$$\lambda_p = \begin{bmatrix} \lambda_1 \\ \lambda_2 \\ \lambda_3 \\ 0 \end{bmatrix}. \tag{10}$$

The null-space solution of the Jacobian matrix as calculated from the relation is as follows:

$$j\lambda_n = 0, \lambda_n = \begin{bmatrix} \lambda_{n1} \\ \lambda_{n2} \\ \lambda_{n3} \\ \lambda_{n4} \end{bmatrix}. \tag{11}$$

https://doi.org/10.1017/S0263574713001288 Published online by Cambridge University Press

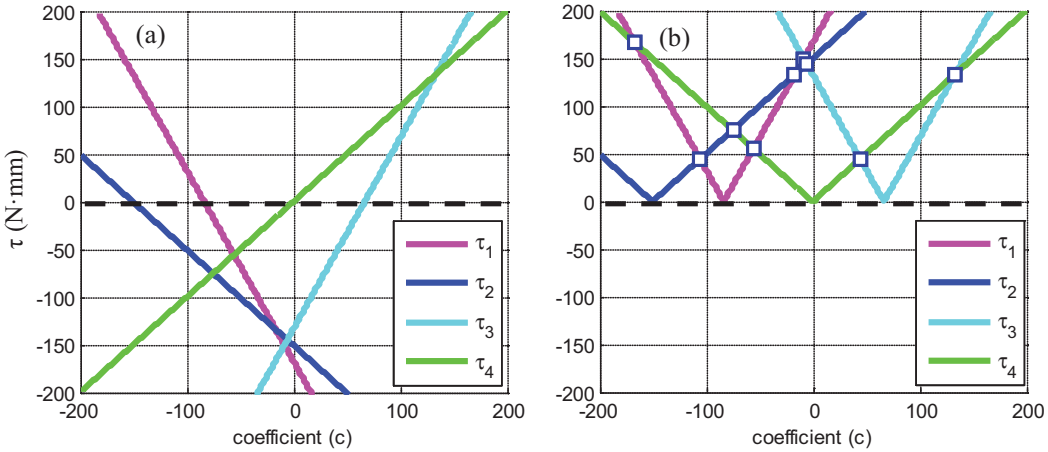

Fig. 4. (Colour online) Null-space solution according to the coefficient: (a) torque and (b) the absolute value of torque. Black dashed lines indicate the point of zero torque, and vertices denote the intersection point of torque ranges searched.

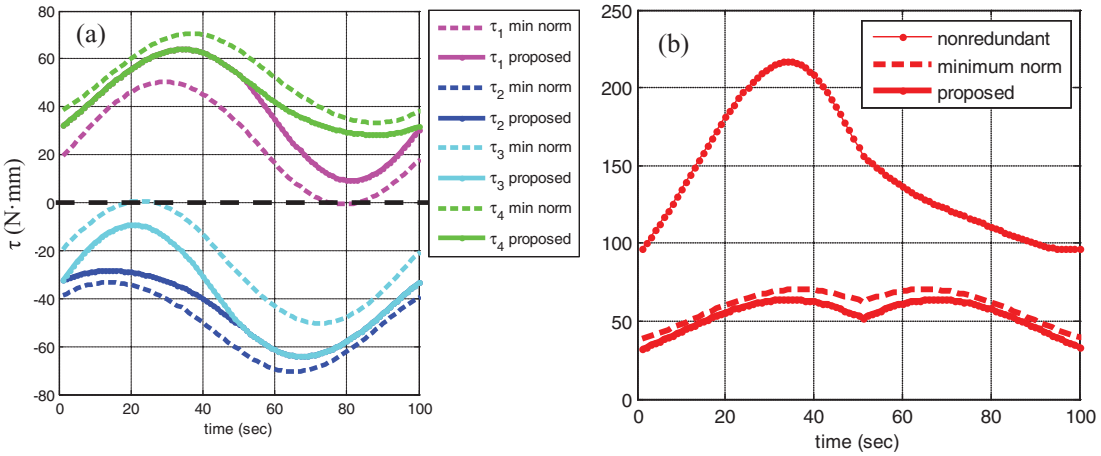

Fig. 5. (Colour online) Actuator torque while the PKM tracks the predefined circular trajectory: (a) torque of four actuators for the minimum-norm method and the proposed method and b) minmax values of the actuator torque ($|\lambda_i|$) for the non-redundant case, the minimum-norm method, and the proposed method. (Note: non-redundant case in (b) is not included in (a).)

Note that we determine the particular solution uniquely and change the null-space solution by using a constant co-efficient. Figure 4(a) shows null-space solutions based on changes in the constant coefficient. As the objective of the optimization is to minimize the magnitude of the maximum torque, we perform absolute operations for all torque ranges, as shown in Fig. 4(b). We then search intersection vertices to identify an optimal solution that can minimize the maximum torque. It is important to note that because the lines in Fig. 4(b) are linear, we can find intersection vertices easily by calculating a series of algebraic equations.

Figure 5 shows the results for the proposed algorithm. Figure 5(a) shows the results for actuator torque for the minimum-norm method and the proposed algorithm. The proposed algorithm reduces peak torque values sharply. Figure 5(b) provides a comparison of the results for the non-redundant case of the maximum torque, the minimum-norm method, and the proposed algorithm, and Table II summarizes the values. The proposed algorithm reduced the maximum torque by 70.5% and 9.18%, relative to the non-redundant case and the minimum-norm method, respectively. This suggests that the proposed algorithm can reduce energy consumption and the number of actuators in the design state.

https://doi.org/10.1017/S0263574713001288 Published online by Cambridge University Press

Table II. Comparison of the maximum torque for the 2-RRR PKM.

	Non-redundant	Minimum-norm	Proposed
Max. torque (N·mm)	216.9	70.48	64.01
Rate (%)	339	110	100

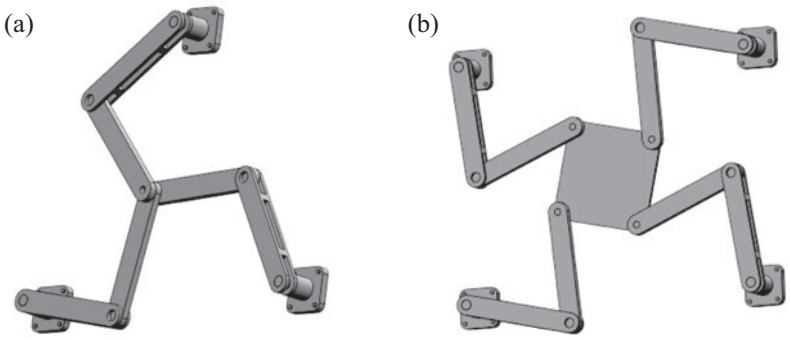

Fig. 6. Redundantly actuated (a) 3-RRR and (b) 4-RRR PKMs. Note the end-effector of 3-RRR PKM has zero size.

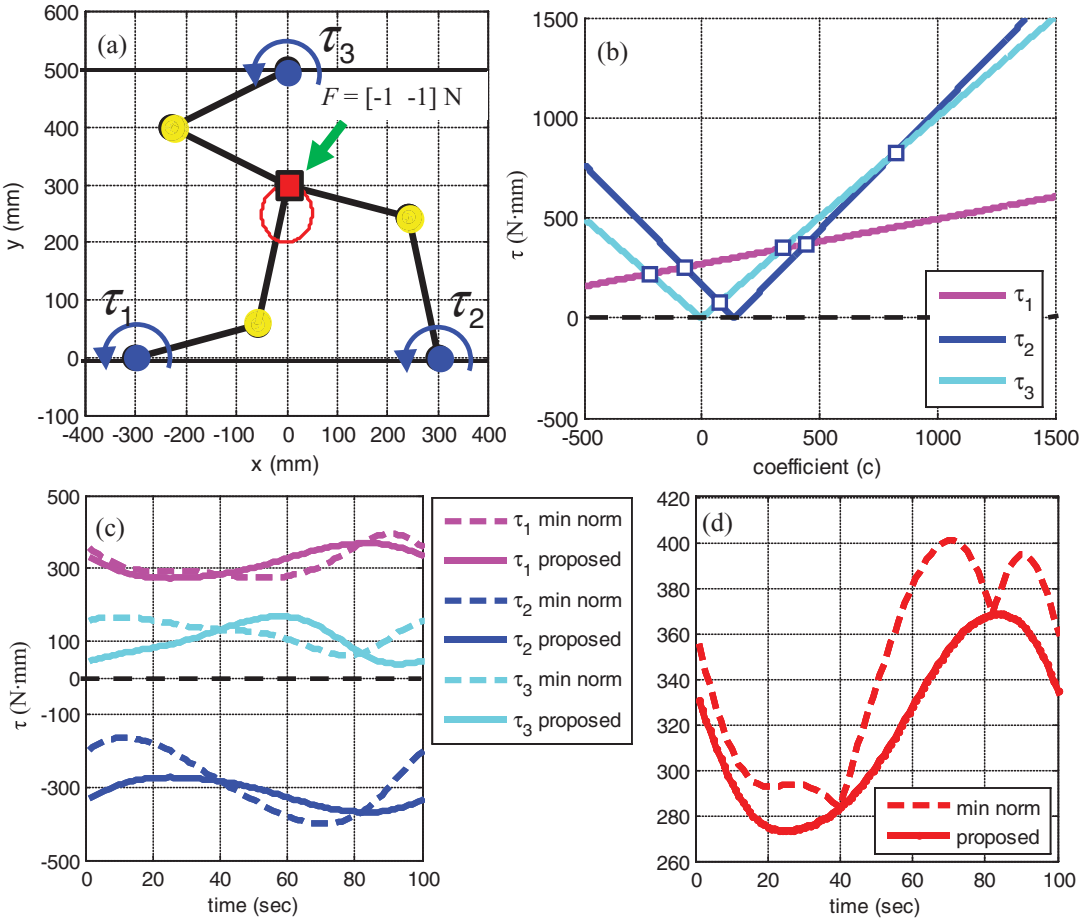

Fig. 7. (Colour online) 3-RRR redundant PKM: (a) the trajectory and external force, (b) absolute values of the null-space solution according to the coefficient, (c) the torque of three actuators when the end-effector tracks the pre-defined trajectory, and (d) the minmax value of actuator torque ($|\lambda_i|$). Lengths of links are 250 mm and distances between actuators are 600 mm.

https://doi.org/10.1017/S0263574713001288 Published online by Cambridge University Press

Table III. Comparison of the maximum torque between 3-RRR and 4-RRR PKMs.

PKM		Maximum torque (N·mm)	Reduction rate (%)
3-RRR	Minimum-norm	400.9	100
	Proposed	368.7	92.0
4-RRR	Minimum-norm	186.6	100
	Proposed	164.7	88.3

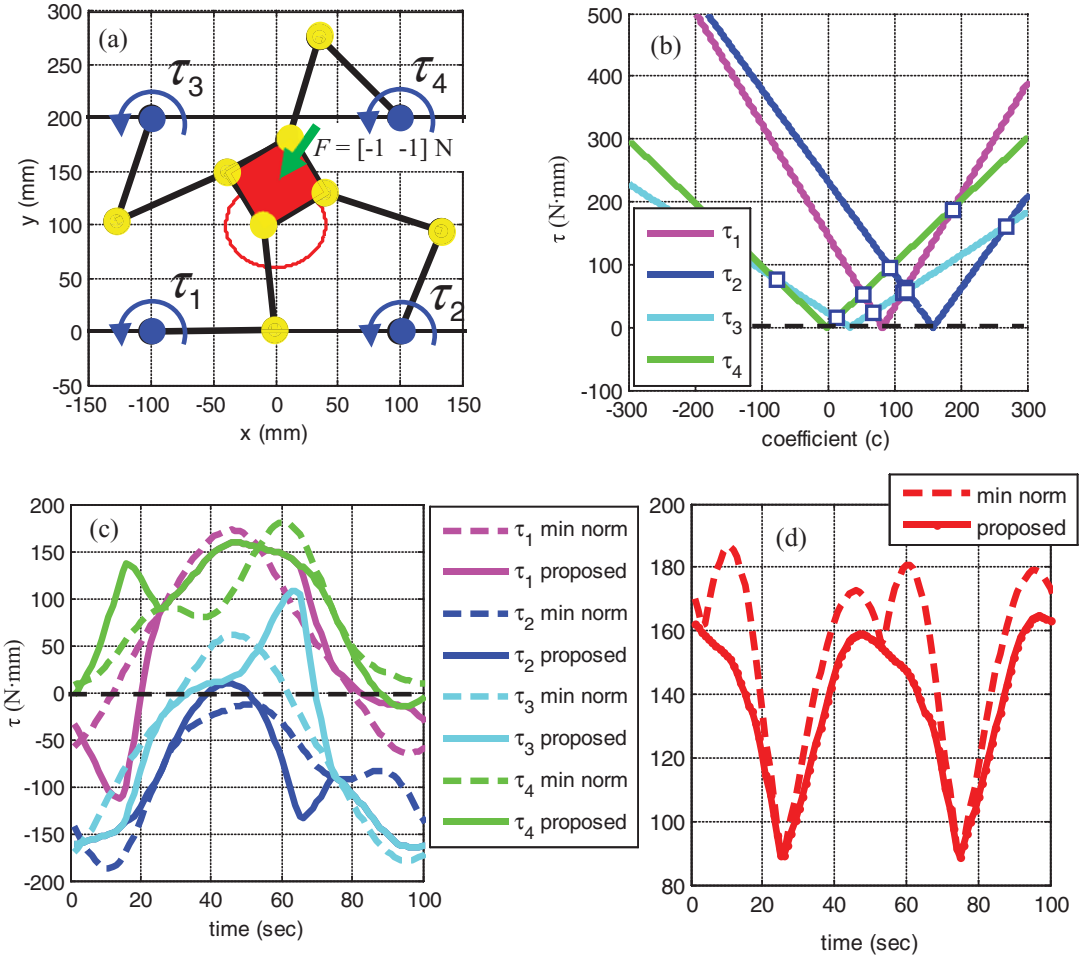

Fig. 8. (Colour online) 4-RRR redundant PKM: (a) the trajectory and external force, (b) absolute values of the null-space solution according to the coefficient, (c) the torque of four actuators when the end-effector tracks the pre-defined trajectory, and (d) the minmax value of actuator torque ($|\lambda_i|$). Lengths of links are 100 mm, edges of the end-effector are 50 mm, and distances between actuators are 200 mm.

4. Case Studies II and III: 3-RRR and 4-RRR PKMs

4.1. Mechanism description

In this section, we analyze two additional cases of redundant PKMs: 3- and 4-RRR PKMs. Figure 6(a) and 6(b) provide a mechanical description of these PKMs. Each leg of the mechanism is composed of RRR chains. Note that the 3-RRR PKM uses three actuators to achieve a 2-DOF motion and 4-RRR PKM uses four actuators to achieve a 3-DOF motion. We calculate the Jacobian matrix based on Screw theory by using the same procedure as in Section 3.2 and thus omit the details of the procedure in this section.

https://doi.org/10.1017/S0263574713001288 Published online by Cambridge University Press

4.2. Torque distribution results

We perform torque distribution by using the proposed algorithm in Section 2. Figures 7 and 8 show the simulation results for 3- and 4-RRR PKMs, respectively. As shown in these figures, the proposed algorithm reduces the resulting maximum torque. Table III compares the proposed algorithm with the minimum-norm method, and the results indicate that the proposed algorithm reduces maximum torque by 8% and 11.7% for 3- and 4-RRR PKMs, respectively.

5. Conclusions

This paper proposes a new torque distribution method for minimizing the peak value of actuator torque for redundant PKMs. We use an optimized null-space solution based on a simple vertex search method with a particular solution for a non-redundant case. We provide three case studies considering 2-, 3-, and 4-RRR redundant PKMs for the analysis and compare the resulting actuator torque with minimum-norm solutions based on the pseudo-inverse of the redundant Jacobian matrix. The results indicate that the proposed algorithm can reduce the minmax torque effectively for 2-, 3- and 4-RRR redundant PKMs, while the reducing efficiency is dependent on the working trajectory.

The proposed algorithm has a limitation. Because it uses a particular solution for a non-redundant case, there is no particular solution in a singular configuration for a non-redundant case. Therefore, the proposed torque distribution method should be used only for non-singular regions. Despite this limitation, this simple and fast algorithm can be used to control energy consumption by redundant PKMs in an efficient manner. Future research should extend the proposed algorithm to spatially redundant PKMs.

Acknowledgements

This research was supported by 2011 Yeungnam Research grant.

References

1. T. Seo, D. S. Kang, H. S. Kim and J. Kim, "Dual servo control of a high-tilt 3-DOF micro parallel positioning platform," *IEEE-ASME Trans. Mechatronics* **14**(5), 616–625 (2009).
2. D. Lee, J. Kim and T. Seo, "Optimal design of 6-DOF eclipse mechanism based on task-oriented workspace," *Robotica* **30**(7), 1041–1048 (2012).
3. W. In, S. Lee, J. I. Jeong and J. Kim, "Design of a planar-type high speed parallel mechanism positioning platform with the capability of 180 degrees orientation," *CIRP Ann. Manuf. Technol.* **57**(1), 421–424 (2008).
4. H. Shin, S. Lee, J. I. Jeong and J. Kim, "Antagonistic stiffness optimization of redundantly actuated parallel manipulators in a pre-defined workspace," *IEEE/ASME Trans. Mechatronics* **18**(3), 1161–1169 (2013).
5. J. Jeong, D. Kang, Y. M. Cho and J. Kim, "Kinematic calibration for redundantly actuated parallel mechanism," *J. Mech. Des. Trans. ASME* **126**(2), 307–318 (2004).
6. D. Jeon, K. Kim, J. I. Jeong and J. Kim, "A calibration method of redundantly actuated parallel mechanism machines based on projection technique," *CIRP Ann. Manuf. Technol.* **59**(1), 413–416 (2010).
7. S. Kock and W. Schumacher, "A Parallel X-Y Manipulator with Actuation Redundancy for High-Speed and Active-Stiffness Applications," *Proceedings of the IEEE International Conference on Robotics and Automation, Leuven, Belgium* (1998) pp. 2295–2300.
8. D. I. Park, S. H. Lee, S. H. Kim and Y. K. Kwak, "Torque distribution using a weighted pseudoinverse in a redundantly actuated mechanism," *Adv. Robot.* **17**, 807–820 (2003).
9. H.-S. Shim, T. Seo and J. W. Lee, "Optimal torque distribution method for a redundant 3-RRR parallel robot using a geometrical analysis," *Robotica* **31**(4), 549–554 (2013).
10. S. Kim, Minimum Consumed Energy Optimized Trajectory Planning for Redundant Parallel Manipulator, *Ph.D. Thesis* (Seoul National University, 2010).
11. S. Ma, S. Hirose and D. N. Nenchev, "Improving local torque optimization techniques for redundant robotic mechanisms," *J. Robot. Syst.* **8**(1), 75–91 (1991).
12. K. Suh and J. Hollerbach, "Local Versus Global Torque Optimization of Redundant Manipulators," *Proceedings of the IEEE International Conference on Robotics and Automation*, Raleigh, NC, USA (1987) pp. 619–624.
13. A. A. Maciejewski, "Real-Time SVD for the Control of Redundant Robotic Manipulators," *Proceedings of the IEEE International Conference on Systems Engineering*, Dayton, OH, USA (1989) pp. 549–552.
14. S. B. Nokleby, R. Fisher, R. P. Podhorodeski and F. Firmani, "Force capabilities of redundantly-actuated parallel manipulators," *Mech. Mach. Theory* **40**(5), 578–599 (2005).
15. J. Wu, J. Wang and L. Wang, "A comparison of two planar 2-DOF parallel mechanisms: one with 2-RRR and the other with 3-RRR structures," *Robotica* **28**(6), 937–942 (2010).

16. Y. K. Yong and T.-F. Lu, "Kinetostatic modeling of 3-RRR compliant micro-motion stages with flexure hinges," *Mech. Mach. Theory* **44**(6), 1156–1175 (2009).
17. J. Wu, J. Wang, L. Wang and Z. You, "Performance comparison of three planar 3-DOF manipulator with 4-RRR, 3-RRR, and 2-RRR structure," *Mechatronics* **20**(4), 510–517 (2010).
18. J. Duffy, *Statics and Kinematics with Application to Robotics* (Cambridge University Press, Cambridge, UK, 1996).
19. G. Strang, *Introduction to Linear Algebra* (Wellesley Cambridge Press, 2003).
20. J. H. Choi and J. W. Lee, "Kinematic Analysis and Drive of 3DOF Parallel Manipulator," *Proceedings of the Joint Symposium of the Sister University of Mechanical University*, Nagasaki, Japan (2012) pp. 73–76.
21. M. W. Spong, S. Hutchinson and M. Vidyasagar, *Robot Dynamics and Control* (Wiley, 2005) pp. 73–117.
22. F. C. Park and J. W. Kim, "Singularity analysis of closed kinematic chains," *ASME J. Mech. Des.* **121**(1), 32–38 (1998).

https://doi.org/10.1017/S0263574713001288 Published online by Cambridge University Press